Anal. Bioanal. Electrochem., Vol. 17, No. 6, 2025, 476-496
https://www.doi.org/10.22034/abec.2025.725967

Analytical &
Bioanalytical
Electrochemistry

2025 by CEE
www.abechem.com

Full Paper

Theoretical Analysis of Two-step EEC′ Mechanism in Square-Wave Voltammetry: Application to Water Soluble Redox Systems with Inverted Potentials

Pavlinka Kokoskarova, Sanja Lazarova, Kiro Papakoca, and Rubin Gulaboski*

Faculty of Medical Sciences, "Goce Delcev" University, Stip, Republic of Macedonia

*Corresponding Author, Tel.: +38975331078
E-Mail: rubin.gulaboski@ugd.edu.mk

Received: 1 June 2025 / Received in revised form: 30 June 2025 /
Accepted: 1 July 2025 / Published online: 7 July 2025

Abstract- Electrochemical systems with inverted redox potentials, where the second electron transfer requires less energy than the first one, often challenge conventional interpretations of sequential redox processes in biomolecules and related complexes. These systems commonly produce a single peak under voltammetric conditions, mimicking a concerted two-electron transfer, thereby obscuring the true stepwise nature of the redox transformation. Through theoretical analysis of a two-step electrode process coupled with a regenerative chemical reaction (the so-called EEC′ mechanism), we demonstrate that increasing the rate of the chemical regeneration step significantly alters the voltammetric response. Notably, this enhanced kinetics induces a negative shift in the potential of the second electron transfer process, eventually resolving the two electron transfer events that otherwise appear merged. Square-wave voltammetry simulations of a diffusional EEC′ mechanism reveal that altering the concentration of the regenerative agent "Y" is essential to achieve this resolution under inverted potential conditions. These findings highlight the critical role of chemical kinetics in shaping voltammetric behavior and provide a powerful framework for studying complex redox systems, including biologically relevant cofactors like iron–sulfur clusters, quinones and flavonoids.

Keywords- Electrochemical-catalytic mechanism; Two-step electrode transformation; EEC′ mechanism; Redox systems with inverted potentials; Kinetics of electron transfer

1. INTRODUCTION

Sequential electron transfer is often considered under voltammetric conditions, since it is a fundamental phenomenon that underpins the functionality of numerous water-soluble redox proteins and enzymes, and many other important biomolecules as well [1-3]. The multistep electron transfer processes commonly involve successive transfer of electrons to specific redox-active centers embedded within defined structures of molecules of interest. Among the various physiological roles of sequential electron transfer, its contribution to energy metabolism and electron transport chains is particularly prominent [4]. Proteins involved in cellular respiration, such as cytochromes and iron-sulfur proteins, mediate electron flow through respiratory pathways, ultimately facilitating ATP synthesis-a process vital for maintaining cellular energy homeostasis. Beyond bioenergetics, consecutive electron transfer events are essential in enzymatic catalysis and redox signaling studied in voltammetric conditions [5, 6]. Enzymes including oxidoreductases and peroxidases exploit these processes to catalyze substrate transformations and modulate intracellular redox balance, thereby counteracting oxidative stress and regulating metabolic flux. A comprehensive understanding of the thermodynamics and kinetics of such electron transfer events is crucial for elucidating the structure–function relationships in redox-active proteins and for deciphering the molecular mechanisms governing complex cellular systems [7].

It is already well-documented that voltammetry is a powerful electroanalytical tool widely employed to probe the redox behavior of proteins and other redox-active biomolecules when dissolved, or immobilized on electrode surfaces [8,9]. It serves as an indispensable tool across various scientific domains, including analytical chemistry, materials science, electrocatalysis, and biosensor development. Particularly, voltammetric analysis enables the investigation of different catalytic mechanisms occurring at electrode–solution interfaces [9]. These processes are central to the operation of energy conversion and storage devices, such as fuel cells and batteries, and play a pivotal role in the design of enzyme-based biosensors. Among the most studied electrode mechanisms under voltammetric conditions is the EC' (electrochemical-chemical regenerative) mechanism, wherein the initial oxidized species (Ox) is regenerated via an irreversible chemical reaction between the reduced form (Red) and a regenerating agent (Y). In previous studies, we have characterized both EC' [10] and EEC' [11] mechanisms using square-wave protein film voltammetric methodology that considers electrode transformation of adsorbed state of redox active enzymes. The present work focuses on a diffusional two-electron transfer mechanism coupled to a homogeneous chemical regeneration reaction involving the final product of the second redox step. This work presents, for the first time, a comprehensive theoretical treatment of the EEC' mechanism under conditions of square-wave voltammetry. The model offers a novel analytical framework with significant potential for distinguishing and characterizing redox systems exhibiting inverted potentials-an area previously unexplored in voltammetric analysis of such redox systems. The primary aim is to delineate key qualitative characteristics of this complex electrochemical system. Moreover, a significant part of the work is focused on introducing an experimental approach capable of detecting and characterizing successive electron transfer steps in redox-active proteins and other water-soluble molecules that exhibit "inverted redox potentials"-a condition where voltammetric responses are typically manifested as a single peak due to closely spaced redox events.

2. Mathematical Model

Theoretical consideration of the elaborated diffusional EEC′ mechanism (I) involves a sequential two-step electrochemical transformation of water-soluble molecules (for simplicity, charges are omitted), represented by the following reaction schemes (a)-(c):

$\mathrm{Ox} + e^- \rightleftharpoons \mathrm{Int}$ $(k_{s,1};\ \alpha_1)$ (a)
$\mathrm{Int} + e^- \rightleftharpoons \mathrm{Red}$ $(k_{s,2};\ \alpha_2)$ (b)
$\mathrm{Red} + \mathrm{Y} \rightarrow \mathrm{Int} + \mathrm{S}$ (k_c) (c) (I)

In reaction schemes (a)-(c) of mechanistic pathway (I), the term "Ox" denotes the initial form of the redox-active molecules present as dissolved species in aqueous solutions. The designation "Int" refers to chemically stable intermediate species, formed electrochemically after the first electrode transformation, while "Red" stays for the final product of the electrochemical transformation attained following the second electron transfer step. "Y" signifies the electrochemically inactive substrate (in the range of potentials applied), which selectively and irreversibly reacts with the "Red" species, thereby regenerating the "Int" species. "S" denotes the side products that are not pertinent to the overall mechanism (I) described by sequences (a) to (c). The reactions (a) to (c) of mechanistic pathway (I) adhere to the following conditions:

$\partial c(\mathrm{Ox})/\partial t = D[\partial^2 c(\mathrm{Ox})/\partial x^2]$ (1);
$\partial c(\mathrm{Int})/\partial t = D[\partial^2 c(\mathrm{Int})/\partial x^2] + c(\mathrm{Red}) \times k_c$ (2);
$\partial c(\mathrm{Red})/\partial t = D[\partial^2 c(\mathrm{Red})/\partial x^2] - c(\mathrm{Red}) \times k_c$ (3);
$t = 0, x \geq 0$: $c(\mathrm{Ox}) = c{*}(\mathrm{Ox})$, $c(\mathrm{Int}) = c(\mathrm{Red}) = 0$; (4)
$c(\mathrm{Ox}) + c(\mathrm{Int}) + c(\mathrm{Red}) = c{*}(\mathrm{Ox})$; (5)
$t > 0, x \rightarrow \infty$: $c(\mathrm{Ox}) \rightarrow c{*}(\mathrm{Ox})$; $c(\mathrm{Int}) \rightarrow 0$; $c(\mathrm{Red}) \rightarrow 0$; (6)

For $t > 0$, and $x = 0$, following conditions apply:

$D[\partial c(\mathrm{Ox})/\partial x]_{x=0} = -I_1/(nFA)$ (7)
$D[\partial c(\mathrm{Int})/\partial x]_{x=0} = [(I_1 - I_2)/(nFA)] + c(\mathrm{Red}) \times k_c$ (8)
$D[\partial c(\mathrm{Red})/\partial x]_{x=0} = [I_2/(nFA)] - c(\mathrm{Red}) \times k_c$ (9)
$I_1/nFA = \exp[-\alpha_1\phi_1]\, k_{s,1} \times [c(\mathrm{Ox})_{x=0} - \exp(\phi_1)\, c(\mathrm{Int})_{x=0})]$; (10)
$I_2/nFA = \exp[-\alpha_2\phi_2]\, k_{s,2} \times [c(\mathrm{Int})_{x=0} - c(\mathrm{Red})_{x=0} \exp(\phi_2)]$; (11)
$\phi_1 = (nF/RT) \times (E - E^{\ominus}_1)$ (12)
$\phi_2 = (nF/RT) \times (E - E^{\ominus}_2)$ (13)

Table 1. Definitions of all parameters explored in the computation of square-wave voltammograms of considered electrode mechanism (I)

Symbol of Physical Parameter/Units	**Meaning of the Parameter**	**Definition**
I/A	Intensity of electric current	
n	Number of electrons exchanged in each electrode transfer step	1
A /cm^2	Active area of the working electrode	
$c^{\square}(\mathrm{Ox})/\mathrm{mol\ cm^{-3}}$	Initial molar concentration of redox species Ox present in electrochemical cell	
$c(\mathrm{Ox})_{x=0}$, $c(\mathrm{Int})_{x=0}$ and $c(\mathrm{Red})_{x=0}$ /mol cm^{-3}	Molar concentrations of species "Ox", "Int", and "Red" at given time t, next to the surface of working electrode (distance considered as $x = 0$)	
$c(\mathrm{Y})$ /mol cm^{-3}	Molar concentration of the substrate (regenerative substance) "Y" dissolved in electrochemical cell	
D/cm^{2}s^{-1}	Diffusion coefficient of all electrochemically active species	0.000005 cm^{2}s^{-1}
F/C mol^{-1}	The Faraday constant	96485 C mol^{-1}
$E_{\mathrm{net,p}}$/V	Peak potentials of simulated net square-wave voltammograms	
Ψ	Dimensionless current of simulated square-wave voltammograms	$\Psi = I/[nFAc^{*}(\mathrm{Ox})(Df)^{0.5}]$
Ψ_{f}	Dimensionless forward currents of simulated square-wave voltammograms	
Ψ_{b}	Dimensionless backward currents of simulated square-wave voltammograms	
$\Psi_{\mathrm{net,p}}$	Dimensionless currents of the net-peaks od simulated net square-wave voltammograms	
T/K	Thermodynamic temperature	298 K
t_p/s	Time-duration of a single potential pulse in SWV	
f/Hz	Frequency of the applied pulses in SWV	$f = t_p/2$
α_1, α_2	Electron transfer coefficients related to the first and the second electron step, respectively	
R/J mol^{-1}K^{-1}	Universal gas constant	8.314 J mol^{-1}K^{-1}
Φ	Dimensionless potential	$\Phi = \frac{nF}{RT}\left(E - E^{\phi'}\right)$
E / V	Applied potential	
$E^{\ominus}_1$/ V	Standard redox potential of redox couple Ox/Int	
$E^{\ominus}_2$/ V	Standard redox potential of redox couple Int/Red	
$K_{\mathrm{ET,1}}$ $K_{\mathrm{ET,2}}$	Dimensionless parameters related to the kinetics of first and second electron transfer, respectively	$K_{\mathrm{ET,1}} = k^{\ominus}_{\mathrm{s,1}}/\sqrt{(D \cdot f)}$ $K_{\mathrm{ET,2}} = k^{\ominus}_{\mathrm{s,2}}/\sqrt{(D \cdot f)}$
$k_{\mathrm{s}}^{\ominus}$ / cm s^{-1}	Standard rate constant of electron transfer	
K_{chem}	Dimensionless parameter related to the rate of irreversible regenerative homogeneous chemical reaction	$K_{\mathrm{chem}} = k_{\mathrm{c}}/f$
k_{c} / s^{-1}	Rate constant of irreversible chemical reaction	$k_{\mathrm{c}} = k_{\mathrm{c}}$' x $c(\mathrm{Y})$
k_{c}'/mol^{-1} cm^3 s^{-1}	Real rate constant of irreversible chemical reaction	
E_{sw} / mV	Amplitude of the square-wave pulses	50 mV
dE / mV	Potential increment	10 mV
B	Numerical integration factor	$B = \mathrm{erf}[[K_{\mathrm{chem}}(m)/50)]^{0.5}] - \mathrm{erf}[[K_{\mathrm{chem}}(m-1)/50]^{0.5}]$
$M1$	Numerical integration factor	$M1 = [(j)^{0.5} - (j-1)^{0.5}]$
m	Serial number of the time intervals in SWV	

The meaning of all symbols related to the parameters referred in equations (1)-(13) is given in Table 1. The entire MATHCAD file containing all parameters and equations that are seen as analytical solution of this mechanism is provided in the Supplementary Material file of this work.

2.1. Parameters influencing the features of simulated square-wave voltammograms

In the context of this mechanism, the features of the simulated square-wave voltammograms depend not only on the parameters of the potential waveform, such as the pulse amplitude (E_{sw}) and the step potential (dE), but also on the temperature and the electron transfer coefficients associated with the two electrochemical steps (α_1 and α_2). Additionally, the behavior of the system is affected by three dimensionless kinetic parameters, i.e. $K_{ET,1}$, $K_{ET,2}$, and K_{chem}. The parameters $K_{ET,1}$ and $K_{ET,2}$ corresponds to the kinetics of the first and second electron transfer (ET) steps, respectively, and are defined as $K_{ET,1} = k^{\ominus}_{s,1}/[\sqrt{(D \cdot f)}]$ and $K_{ET,2} = k^{\ominus}_{s,2}/[\sqrt{(D \cdot f)}]$. In these two equations defining $K_{ET,1}$ and $K_{ET,2}$, $k^{\ominus}_{s,1}$ and $k^{\ominus}_{s,2}$ are the standard heterogeneous rate constants for the respective steps, D is the diffusion coefficient (assumed equal for all species involved), and f is the applied square-wave frequency. These parameters ($K_{ET,1}$ and $K_{ET,2}$) reflect the relative rate of electron transfer steps compared to the rate of the diffusion of electrochemically active species. The third dimensionless kinetic parameter, K_{chem}, characterizes the rate of the homogeneous regenerative (catalytic) step, and is defined as $K_{chem} = k_c' \times c(\mathrm{Y})/f$, where k_c' is the second-order rate constant of the regenerative reaction (with units $\mathrm{s^{-1}cm^3mol^{-1}}$), and c(Y) is the molar concentration of the regenerating species Y present in excess in electrochemical cell. This parameter portrays the rate of the homogeneous catalytic reaction relative to the timescale imposed by the square-wave frequency. It is worth to note that, since each of the mentioned three dimensionless parameters ($K_{ET,1}$, $K_{ET,2}$ and K_{chem}) is function of the square-wave frequency f, the frequency simultaneously modulates the effective kinetics of all steps involved in this particular mechanism. This consideration is quite important, as time-based analysis can frequently lead to misinterpretations when applied to this specific mechanism.

3. RESULTS AND DISCUSSION

3.1. Brief insights into limiting situation of EEC′ mechanism in square-wave voltammetry

Although several two-step "diffusional" mechanisms have been theoretically examined under square-wave voltammetry (SWV) conditions [12-14], the sequential diffusional EEC' mechanism addressed in this work has not been the subject of theoretical investigation in SWV so far. In our study published in 2011 [11], we presented key theoretical results for the EEC' mechanism, but analyzed within the framework of protein-film voltammetry conditions. In analyzing the current diffusional EEC' mechanism, it is essential to assess its validity by examining a limiting case governed by the rate of the regenerative chemical reaction associated with the product of the second electron transfer step. When the dimensionless chemical kinetic parameter K_{chem}, which governs the rate of regenerative chemical step following the second electron transfer, is $K_{\mathrm{chem}} < 0.001$, then the considered EEC' mechanism effectively reduces to a simple two-step EE mechanism [9,15]. In voltammetric analysis, the two-step diffusional EE mechanism describes a process in which an electroactive species undergoes two sequential electron transfer steps, with diffusion controlling the transport of each species to and from the electrode. For the second electron transfer step to appear as a well-defined peak in the voltammograms, certain preconditions must be met. Most importantly, there must be sufficient potential separation between the formal (or standard) potentials of the two steps, usually on the order of 150 mV or more, to resolve them under typical scan rates applied in SWV [12-16]. If both electron transfer steps are too close in potential, the corresponding peaks may merge or appear as a single broadened wave [13]. Additionally, the intermediate species "Int", created upon the first electrode transformation, must be chemically stable on the voltammetric timescale, thus avoiding rapid dimerization or follow-up chemical reactions that would deplete it before the second electron transfer can occur. When considered under conditions of square-wave voltammetry, several key parameters govern the behavior of such systems and determine the features observed in the resulting voltammograms. Central among these are the kinetics of both electron transfer steps, described in the model by the dimensionless kinetic parameters $K_{\mathrm{ET},1} = k^{\ominus}_{s,1}/[\sqrt{(D \cdot f)}]$ and $K_{\mathrm{ET},2} = k^{\ominus}_{s,2}/[\sqrt{(D \cdot f)}]$. These two dimensionless kinetic parameters ($K_{\mathrm{ET},1}$ and $K_{\mathrm{ET},2}$) integrate the electron transfer kinetics with the diffusion rates of electrochemically active species, relative to the timescale defined by the square-wave (SW) frequency at each applied SW potential pulse. If both electron transfer steps are fast, the voltammograms will display reversible behavior, while small values of K_{ET} (commonly at $K_{\mathrm{ET}} < 0.001$) can cause peak broadening or shifting of the positions of the corresponding peaks at potential scale [15]. Figure 1 presents square-wave voltammograms of various simulated scenarios based on different assumed rates for both electron transfer steps. In the so-called "*reversible region*", where K_{ET} is large (typically for log ($K_{\mathrm{ET}} > 0.5$)), electron transfer is rather fast, and the system maintains near-equilibrium conditions. Under these conditions, the forward and backward currents are nearly symmetrical, while the ratio of their peak currents is 1 (Figure 1a). The peak-to-peak separation between cathodic and anodic peaks (ΔEp) is minimal, approaching zero, which indicates that the reduction and oxidation processes occur almost at the same potential. As the system moves into the "*quasi-reversible region*" (intermediate values of K_{ET}, typically between 0.1 and 5), the electron transfer begins to lag behind the applied potential waveform. Consequently, both the forward and backward current peaks begin to shift away from each other. The reduction peak (the forward peak in this work) moves toward more negative potentials, while the backward peak (re-oxidation in the current work) shifts toward more positive potentials (Figure 1b).

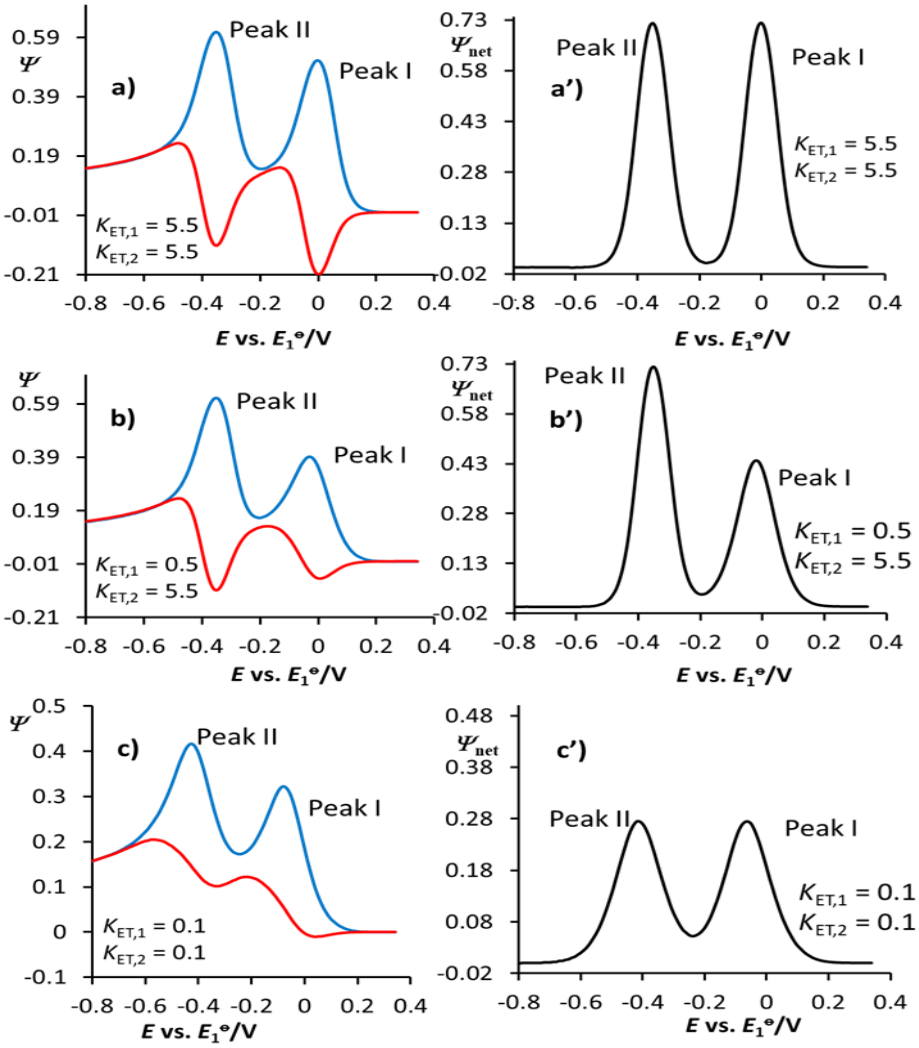

Figure 1. Forward and backward (a–c) and corresponding net (a′–c′) current–potential profiles of square-wave voltammograms of the diffusional EEC′ mechanism simulated under varying values of the dimensionless kinetic parameters corresponding to the first and second electron transfer steps, $K_{ET,1}$ and $K_{ET,2}$, respectively. The simulations were conducted under conditions approximating the absence of a regenerative chemical reaction (with K_{chem} = 0.0001), and assuming electron transfer coefficients of 0.5 for both electrode steps. The other simulation parameters were as follows: square-wave frequency f = 10 Hz, square-wave amplitude E_{SW} = 50 mV, potential increment dE = 10 mV, and temperature T = 298 K. Equal number of exchanged electrons (n = 1) and equal diffusion coefficients were assumed for all electroactive species, set at $D = 5\times10^{-6}$ cm² s⁻¹. The potential difference between the two electrochemical steps was fixed at 300 mV. The magnitudes of the dimensionless kinetic parameters $K_{ET,1}$ and $K_{ET,2}$ are given in the charts. Starting potential was set to + 0.35 V.

This results in an increase in potential separation between the both peaks. In the quasireversible region, the current amplitudes also change: the forward peak current decreases while the backward peak becomes less defined and may even disappear entirely as the system becomes more irreversible. Finally, in the "*irreversible region*" ($K_{ET} < 0.1$), electron transfer is so sluggish that the redox reaction cannot keep up with the changing potential.

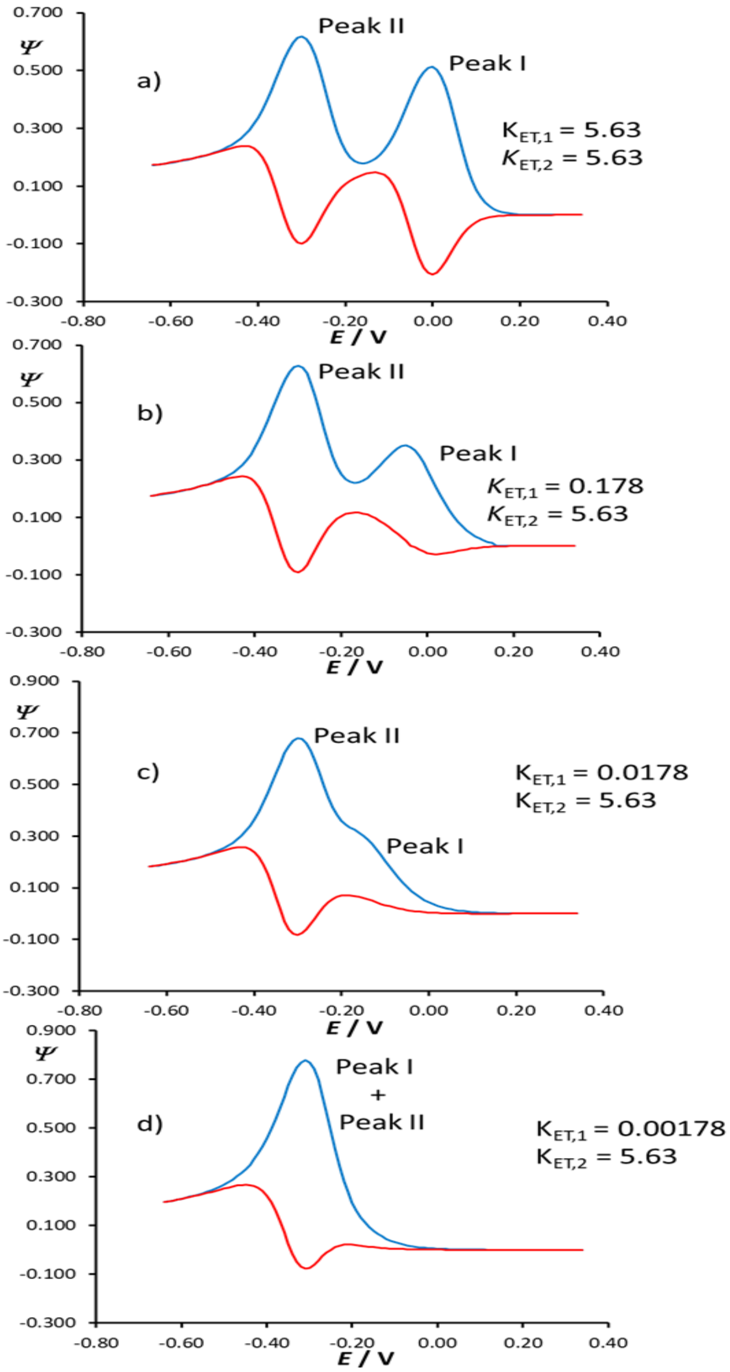

Figure 2. Forward and backward current–potential curves of square-wave voltammograms illustrating their evolution as a function of the dimensionless rate constant for the first electron transfer step. The dimensionless rate parameter for the second electron transfer step ($K_{ET,2}$) was fixed at 5.63, while all other simulation conditions were identical to those described in Figure 1. The magnitudes of $K_{ET,2}$ are given in the graphs.

This condition leads to a highly asymmetric voltammogram in which the forward peak dominates, while the backward current is negligible or completely absent (Figure 1c). Peak currents are diminished overall, and the forward peak shifts further in the direction of the applied potential to overcome kinetic barriers. The peak-to-peak separation becomes very large or undefined due to the loss of the backward peak (Figure 1c). At this stage, it is noteworthy to elaborate one specific scenario, in which the kinetics associated with the first peak become increasingly sluggish, whereas the second peak exhibits nearly reversible behavior across all applied scan rates. This kinetic disparity results in a progressive shift of the first peak toward more negative potentials as the magnitude of the rate constant $K_{\mathrm{ET},1}$ decreases (see Figure 2a–c). In contrast, the characteristics of the second peak remain largely unaffected. At sufficiently low values of $K_{\mathrm{ET},1}$, the first peak merges with the second one, ultimately giving rise to a single, peak as the existing one in the voltammetric profile (see Figure 2d).

Another critical parameter of this mechanism are the electron transfer coefficients linked to both electron transfer steps (α_1 and α_2), which describe the symmetry of the energy barrier for the corresponding electron transfer [9,15]. This affects the shape and position of the peaks, particularly under quasireversible conditions (see Figure 3). In the region of sluggish electron transfers, conventional methods used for reversible systems to determine kinetic parameters are no longer applicable. However, it is still possible to extract valuable kinetic information, particularly the electron transfer coefficient (α), which reflects the symmetry of the energy barrier for electron transfer. One effective approach for evaluating electron transfer coefficient α in redox systems characterized with slow electron transfer rate involves analyzing the peak potential shift with respect to the logarithm of frequency [17]. In SWV, since the frequency influences the effective scan rate, plotting the peak potential (E_p) against $\log(f)$ can yield a linear relationship under irreversible conditions. From the slope of this plot, α can be extracted using the equation derived using the methodology described in [17].

As previously mentioned in the introduction to this section, the potential separation (ΔE) between the two voltammetric peaks is a critical parameter that determines the shape of the final voltammetric response in the context of the considered EEC' mechanism. This is clearly illustrated in Figure 4, which presents simulated voltammetric patterns for different magnitudes of potential separation between the two electron transfer processes. When the energy of the second electron transfer (ΔE) is less than -150 mV relative to the first electron transfer, two distinct peaks are observed in the square-wave voltammetric output (Figure 4a). If the potential separation (ΔE) falls between -50 mV and -120 mV, a broad peak with a shoulder-like feature appears in the voltammograms (Figure 4b). Conversely, when the energies of both electron transfer processes are close (ΔE between 0 mV and -30 mV), a single peak emerges in the voltammetric response, masking the individual contributions of both electron transfers (Figure 4c). Indeed, the scenario depicted in Figure 4c warrants closer examination, as it is necessary to determine whether the observed single peak in a given experimental scenario result from a single one-step two-electron transfer, or from the sequential transfer of two electrons in closely spaced steps with similar energies of occurrence.

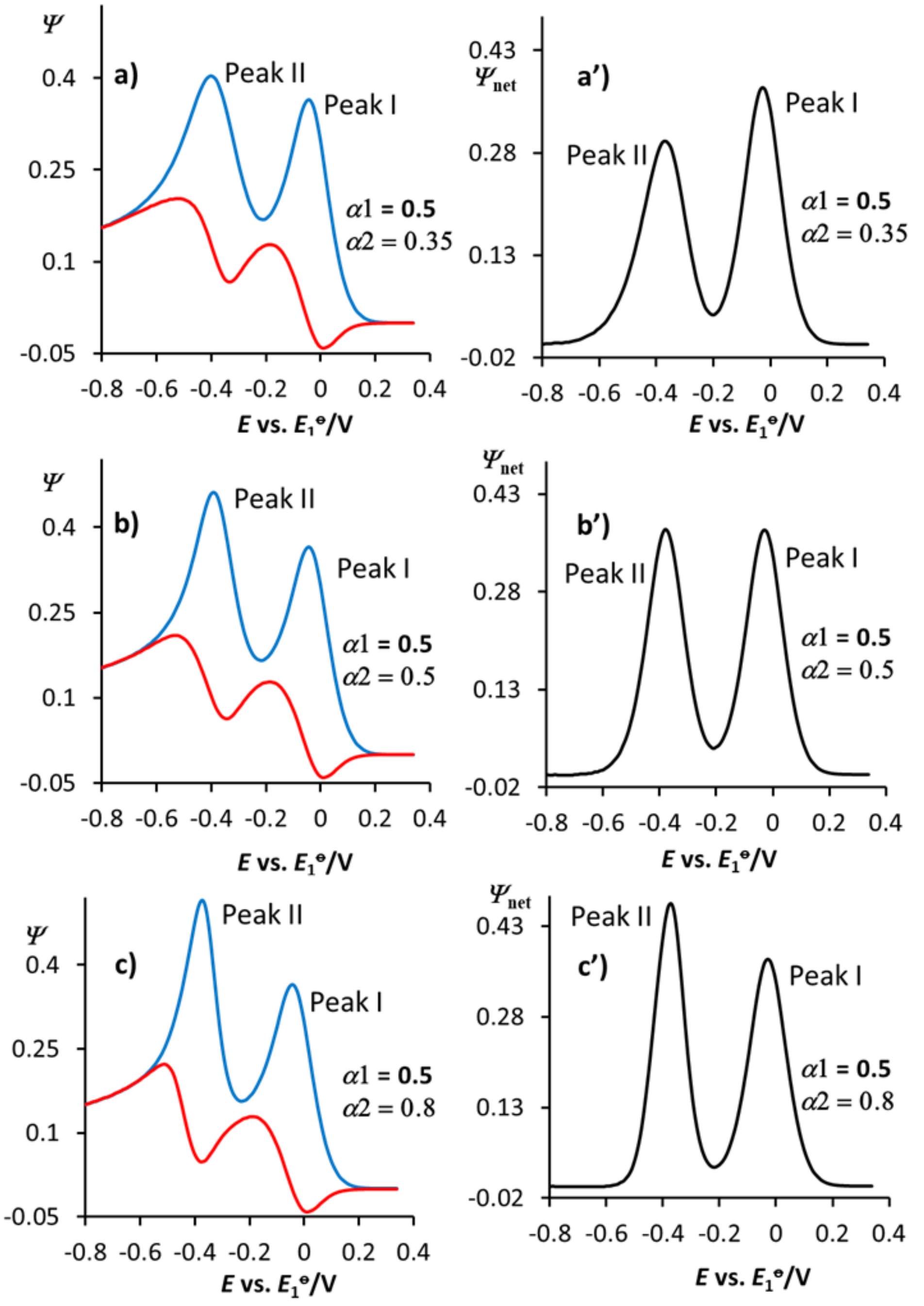

Figure 3. Forward and backward (a–c) as well as net (a′–c′) current–potential curves of square-wave voltammograms simulated for the diffusional EEC′ mechanism under varying values of both electron transfer coefficients (magnitudes of $\alpha 1$ and $\alpha 2$ are given in the graphs). The simulations were performed assuming equal values for the dimensionless rate parameters of both electron transfer steps ($K_{ET,1} = K_{ET,2} = 0.224$). All other simulation parameters were identical to those described in Figure 1.

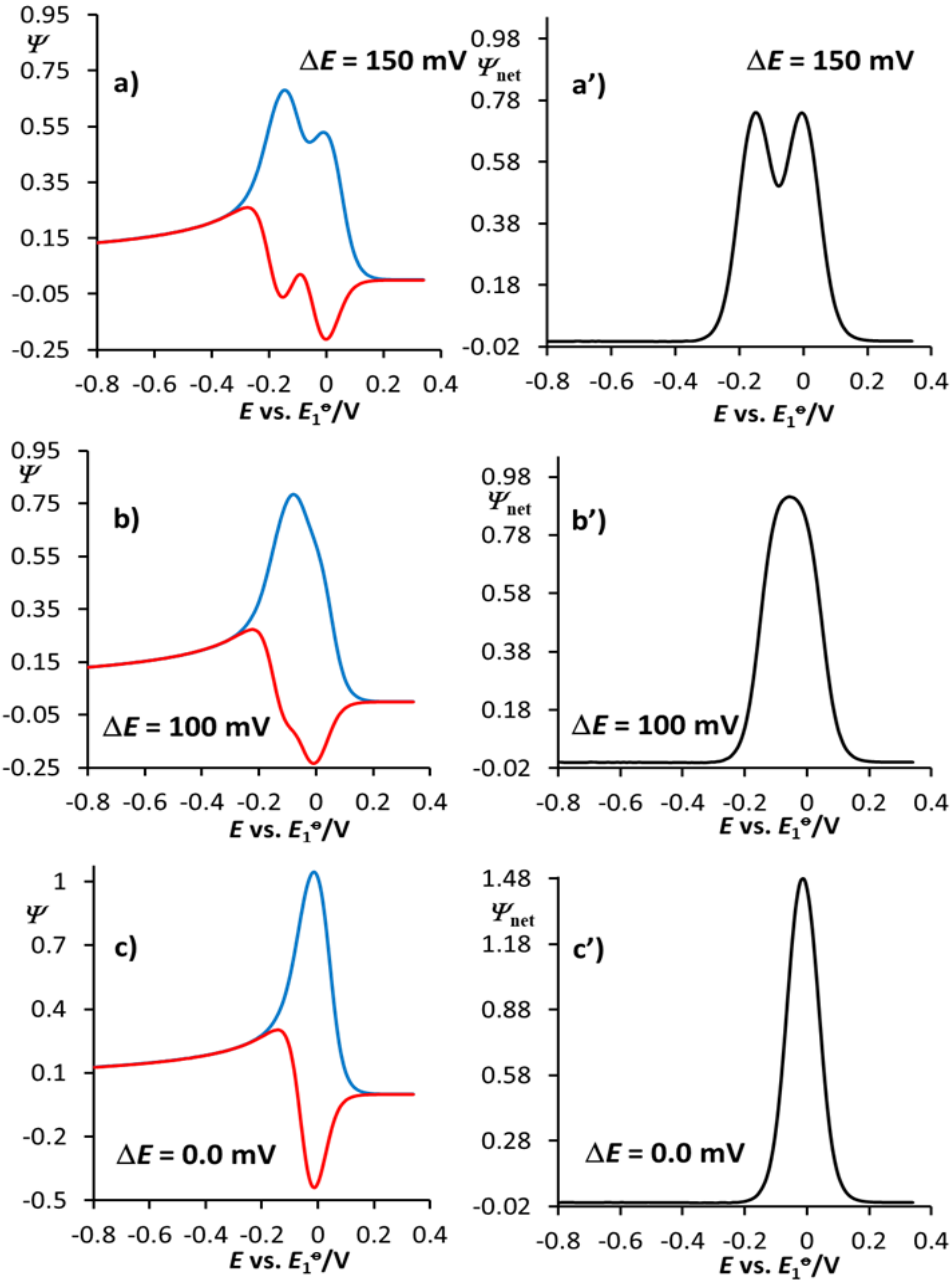

Figure 4. Forward and backward (a–c) and net (a′–c′) current–potential curves of square-wave voltammograms simulated for three different magnitudes of the potential difference (ΔE) between the first and the second electron transfer step (values of (ΔE are given in the graphs). The calculations were performed assuming equal values for the dimensionless rate parameters of both electron transfer steps ($K_{ET,1} = K_{ET,2} = 10$). All other simulation parameters were identical to those described in Figure 1.

3.2. Major effects of regenerative reaction to the features of EEC′ mechanism in SWV

The regenerative (or electrocatalytic) mechanism considered in the current scenario leads to regeneration of intermediate redox active species “Int” via irreversible and selective chemical reaction between the product of second electron transfer step “Red” and a given substrate “Y”. Since the regenerative chemical reaction “consumes” the final product “Red’, it contributes to regenerating the interim electroactive species “Int”, thus enabling its further electrochemical reduction in the current-measuring time frame of potential SW pulses. This sequence of events will influence the voltammetric profiles of considered EEC′ mechanism in a rather specific manner [15]. The regeneration of “Int” through the chemical reaction of “Red” with “Y” leads to a continuous resupply of reducible species near the electrode surface. As a result, the cathodic current increases beyond what would be expected for a simple diffusion-controlled redox couple. The higher the rate of regeneration step, the higher the catalytic current observed during the forward scan. Oppositely, the backward scan (or anodic scan in our consideration) shows an oxidation peak corresponding to the re-oxidation of “Red”. Since in the electrochemical-catalytic mechanism much of “Red” is consumed chemically by “Y”, less “Red” species will be available for oxidation during the reverse scan. This leads to a diminished or even absent reverse peak, particularly under fast chemical kinetics. Under certain experimental conditions, particularly at slow scan rates, a steady-state current may be observed in EC' mechanisms [8,18]. This condition is characterized by a plateau in the current-potential response rather than a peak, indicating that the rate of electrochemical reduction is balanced by the rate of mass transport and chemical regeneration of “Int” redox species. Steady-state is typically achieved a) when the scan rate is low enough that diffusion layers are fully developed, or b) the catalytic reaction Red + Y → Int proceeds at a very large rate sufficient to maintain a constant supply of “Int” redox species at the electrode surface [19]. Under steady-state, the catalytic current becomes independent of time and instead depends on the rate constant of the chemical step and the concentration of the reagent “Y” only [20]. All these phenomena, associated with the presence of two well-separated peaks in the considered EEC' mechanism, are clearly illustrated in the voltammograms presented in Figures 5a and 5b. Figures 5a-b showcase the evolution of both forward and reverse voltammetric current profiles under the influence of an increasing rate of the regenerative reaction (from patterns 5a towards patterns on 5b). Indeed, since the regenerative chemical reaction is not associated with the first voltammetric peak (Peak I), its characteristics remain unaffected by variations in K_{chem}. In this sequence of events, only the characteristics of the second voltammetric process (Peak II) exhibit specific changes with increasing K_{chem}, as is typical for a well-elaborated electrochemical-regenerative mechanism [9,15,20].

Figure 6 displays the net square-wave voltammograms corresponding to the forward and reverse voltammetric curves shown in Figure 5a-b. Since Peak I remains unaffected by the rate of the regenerative chemical reaction, only Peak II exhibits a progressive increase in magnitude with increasing values of the chemical parameter K_{chem}. Furthermore, for $K_{\mathrm{chem}} > 0.5$, Peak II undergoes a shift toward more negative potentials as K_{chem} increases. As previously reported in [15], the net peak potential ($E_{\mathrm{net,p}}$) varies linearly with $\log(K_{\mathrm{chem}})$, where the slope of this dependence is governed by the electron transfer coefficient, α. This distinctive behavior of the net peak potential in square-wave voltammetry as a function of the regenerative reaction rate constant provides a means to probe the kinetics of the regenerative step, assuming that electron transfer coefficient α and the standard heterogeneous electron transfer rate constant are known [18]. Moreover, the shift in the net SWV peak potential of the second voltammetric process to negative potentials with increasing rate of the regenerative step can be utilized to characterize EE mechanisms in systems with inverted potentials, as will be demonstrated and discussed in more details in the following section of this work.

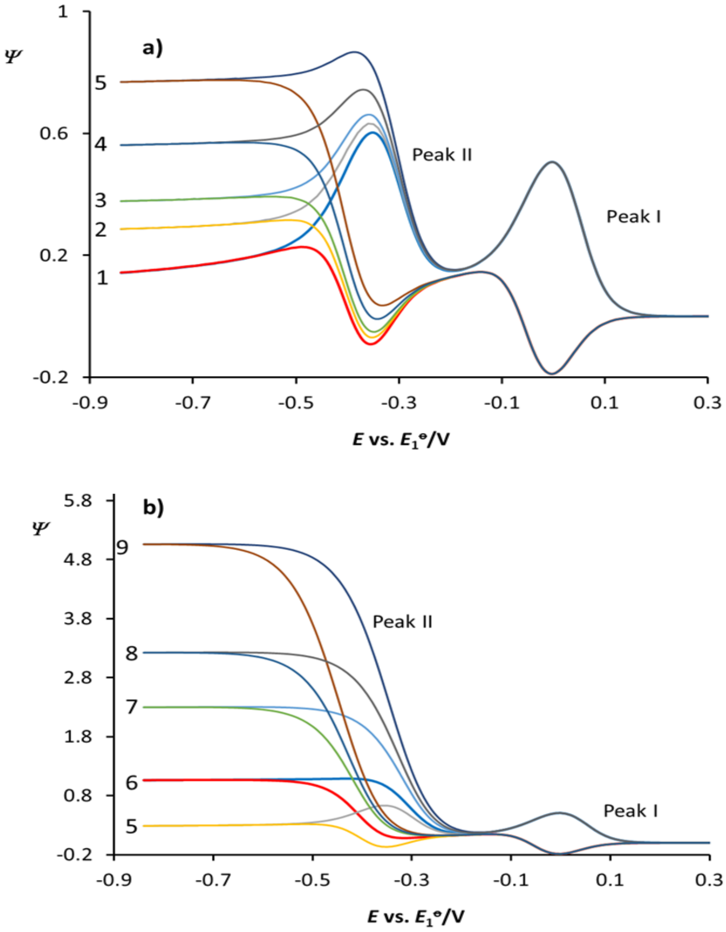

Figure 5. Forward and backward current–potential curves of square-wave voltammograms for the diffusional EEC′ mechanism illustrating their evolution as a function of the dimensionless rate parameter related to the regenerative chemical reaction (K_{chem}). The dimensionless rate parameter for both the first and the second electron transfer step ($K_{\mathrm{ET,1}}$ and $K_{\mathrm{ET,2}}$) were fixed at 2.0. The magnitudes of chemical catalytic rate parameter were as follows: K_{chem} = 0.00001 (1); 0.05 (2) 0.1 (3) 0.25 (4) 0.5 (5-6); 1 (7); 5 (8); 10 (9) and 20 (10). All other simulation conditions were identical to those described in Figure 1. Voltammograms 5 (in pattern a) and 5 (in pattern b) are identical, while the voltammograms shown in pattern b) represent a continuation of those presented in pattern a).

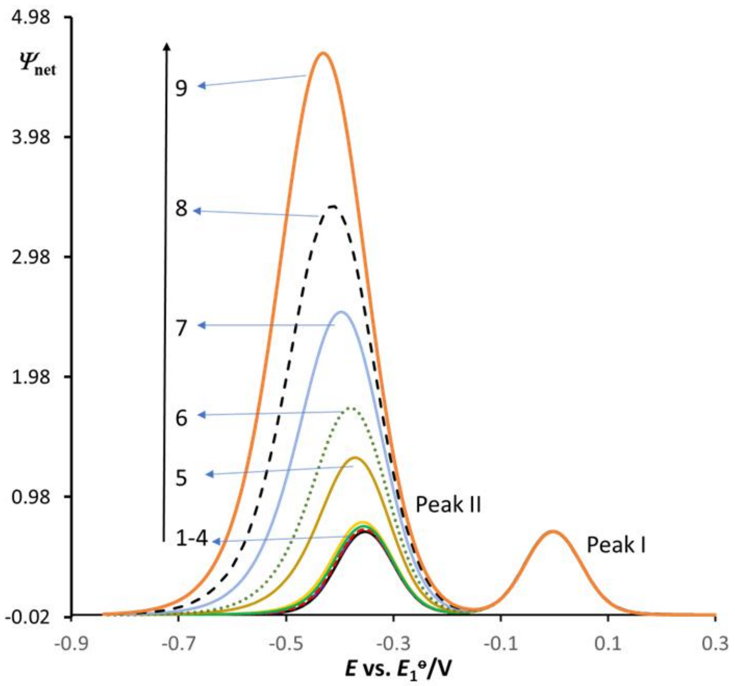

Figure 6. Net current–potential curves of square-wave voltammograms for the diffusional EEC′ mechanism illustrating their evolution as a function of the dimensionless rate parameter related to the regenerative chemical reaction (K_{chem}). Other simulation conditions are same as those in Figure 5

3.3. Exploring the EEC′ mechanism to characterize systems with inverted potentials in SWV

Chemical systems with inverted redox potentials present a fascinating deviation from conventional electrochemical expectations. In conventional redox chemistry, the stepwise reduction of an oxidized species to its fully reduced form typically proceeds through two sequential one-electron transfer steps, often involving the formation of a relatively stable intermediate. In most cases, the second electron transfer requires a higher driving force (i.e., occurs at a more negative potential) than the first one. However, in certain systems exhibiting inverted redox potentials, this trend is reversed: the second reduction, involving the intermediate species, requires less energy and occurs at a more positive potential than the initial reduction step that generated the intermediate species. This counterintuitive behavior has its roots in electronic structure rearrangements, solvation effects, and structural reorganizations that accompany redox processes [21]. The origin of inverted potentials is often associated with systems where redox events induce significant conformational or electronic changes. These changes can stabilize the intermediate (or first reduced form in our mechanism) to such an extent that further redox steps appear anomalously shifted. For instance, in certain transition metal complexes or organic radical systems, electron transfer leads to intramolecular rearrangements or hydrogen bonding that substantially alters thermodynamic stability. Additionally, proton-coupled electron transfer can contribute to potential inversion when protonation alters the electronic environment of the redox-active site [22]. In biochemistry, inverted potential systems are highly relevant. Several metalloenzymes and cofactors, such as those found in respiratory electron transport chains, exploit this phenomenon [23]. A prominent example includes iron–sulfur clusters, where the redox behavior can be inverted depending on protein environment and protonation state [24]. This behavior can be crucial for directionality in electron flow, allowing biological systems to couple energy-requiring and energy-releasing steps efficiently. Similarly, flavonoids and quinones in enzymes often exhibit multiple redox states with unusual potential sequences that support controlled sequential electron transfer [25-27].

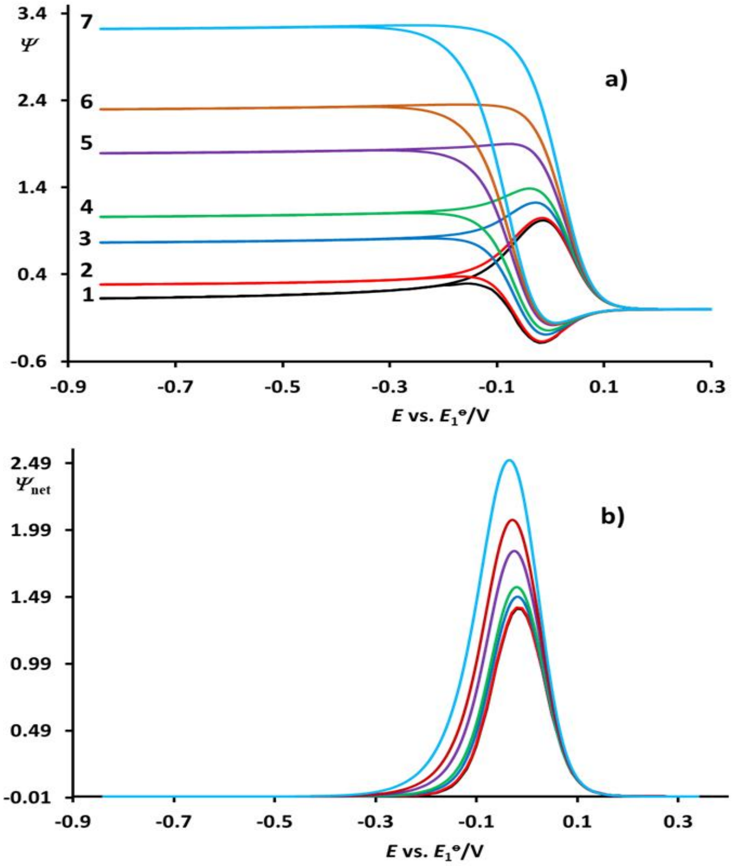

Figure 7. *Scenario of systems with inverted potentials*: Forward and backward (a) and net (b) current–potential curves of square-wave voltammograms for the diffusional EEC′ mechanism illustrating their evolution as a function of the dimensionless rate parameter related to the regenerative chemical reaction (K_{chem}), when dimensionless kinetic parameters of both electron transfer steps fall in region of fast electron transfer ($K_{\mathrm{ET},1} = K_{\mathrm{ET},2} = 10$). The magnitudes of chemical catalytic rate parameter were as follows: $K_{\mathrm{chem}} = 0.0001$ (1); 0.05 (2) 0.5 (3) 1.0 (4) 3.0 (5); 5.0 (6) and 10.0 (7). The potential difference (ΔE) between the first and the second electron transfer step was set to 0.0 mV. Other simulation conditions were same as those in figure 5. The colors of the voltammograms in pattern b) correspond to those of the forward and backward curves shown in pattern a).

The voltammetry of systems with inverted potentials reveals unique signatures. In cyclic voltammetry, such systems may show peak separation that contradicts expected thermodynamic trends or even crossing redox waves if multiple species interconvert via structural rearrangements [28]. Additionally, irreversible or quasi-reversible behavior commonly dominate, reflecting kinetic barriers to conformational changes rather than simple electron transfer. In majority of the experimental cases, however, the systems with inverted potentials are portrayed in a single voltammetric peak [13]. Understanding these patterns requires careful interpretation and, often, the support of computational data to elucidate underlying mechanisms.

In our previous work we have shown that the square-wave voltammetry can provide means to recognize systems with inverted potentials by electrochemical mechanisms in which chemical step contributes to the formation of initial redox species in the so-called "CEE mechanism" [29]. Figure 7 illustrates the voltammetric behavior of a redox system with inverted redox potentials. When the second electron transfer occurs at a lower energy than the first one, both electron transfer steps may appear as a single feature in the voltammetric response, as typical for a concerted two-electron process. Assuming that both electron transfers are electrochemically reversible, as depicted in Figure 7a-b, an increase in the rate of the regenerative chemical step leads to voltammograms that resemble those expected for a classical EC′ mechanism involving a two-electron transfer [15,20]. However, if the second electron transfer in such a scenario occurs within the irreversible or quasireversible regime, an increase in the rate of the regenerative chemical step will shift the peak potential of the second process toward more negative values [10] (Figures 8a-d). This feature is already demonstrated at the Peak II in Figures 5 and 6, and it is a unique for this mechanism. As reported in [8,19], considering the thermodynamics and kinetics effects in an EC′ mechanism, the interplay between the electrochemical and chemical steps significantly influences the features of observed voltammetric response. When considering an overall reduction process as in the current scenario (Ox + e- ⇄ Red), a particularly notable feature is the shift of the peak potential toward more negative as the kinetics of the regenerative chemical step increases. This phenomenon arises from the dynamic coupling between the electron transfer and the subsequent catalytic regeneration of the reactant. As the chemical step becomes faster, the reduced species formed at the electrode is rapidly consumed through its reaction with a regenerative agent "Y", while regenerating the original oxidized form. This swift removal of "Red" prevents its accumulation near the electrode surface, thereby disturbing the local equilibrium between oxidized form and "Red". Keeping in mind the Nernst equilibrium conditions next to the electrode surface, the electrode potential is governed by the ratio of the surface concentrations of "Red" and the "Ox". A lower concentration of "Red" relative to "Ox" shifts this ratio, requiring a more negative potential to maintain or increase the rate of electron transfer necessary to produce more "Red".

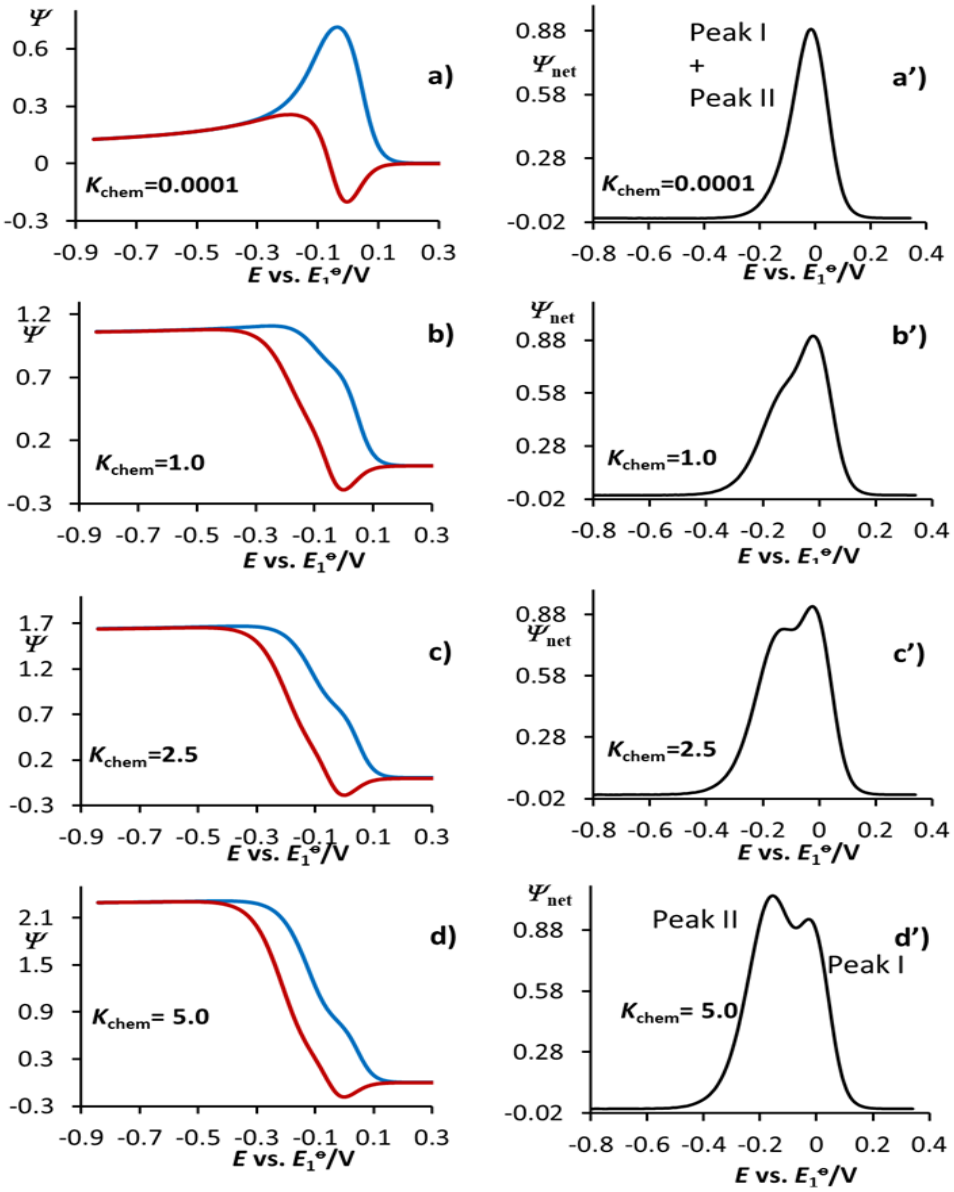

Figure 8. *Scenario of systems with inverted potentials*: Forward and backward (a–d) and corresponding net (a′–d′) current–potential profiles of square-wave voltammograms illustrating their evolution as a function of the dimensionless rate parameter related to the regenerative chemical reaction (K_{chem}). Voltammograms are calculated for the potential difference of $\Delta E = 0$ between the first and the second electron transfer step. Magnitudes of K_{chem} given in the charts. The calculations were performed for $K_{\mathrm{ET,1}} = 2.0$ and $K_{\mathrm{ET,2}} = 0.1$. Other simulation conditions were same as those in Figure 1.

In essence, the system demands a greater driving force to sustain the reduction process in the face of ongoing catalytic consumption of its product. Consequently, the peak potential in voltammetric experiments shifts in the negative direction. This shift reflects the departure from a reversible electrochemical regime, as the fast chemical reaction alters the steady-state conditions at the electrode. The electrochemical response becomes kinetically controlled, and the voltammogram displays both an enhanced current due to the catalytic recycling of the reactant, and a shift in peak position [9,10]. Consequently, the negative shift of the peak potential in such scenario is a direct manifestation of the increasing demand for electron transfer to compensate for the rapid depletion of the reduced species, highlighting the fundamental interplay between kinetics and thermodynamics in EC′ systems. As a result of these phenomena, both electron transfer steps in considered EEC′ mechanism (in scenario of inverted potentials) become increasingly separated, ultimately producing two well-resolved net peaks in the overall SW voltammetric response (see the net patterns in Figures 8c′–d′).

4. CONCLUSION

In this work, it has been demonstrated that the square-wave voltammetry, in combination with mechanistic analysis of the diffusional EEC′ mechanism, offers a powerful approach to dissecting these unusual systems. The square-wave voltammetric response of such mechanisms reveals subtle but significant patterns. When the second electron transfer is thermodynamically more favorable (i.e., occurs at a less negative or even more positive potential), the overall voltammogram is commonly present as a single composite peak, mimicking a concerted two-electron process. However, the apparent simplicity of this response masks a complex interplay of electrochemical and chemical kinetics. Our theoretical analysis shows that increasing the rate of the regenerative chemical step (which rapidly consumes the intermediate reduced species and regenerates the oxidized form) significantly alters the voltammetric profile. Specifically, this enhanced kinetic pathway causes the peak potential associated with the second electron transfer to shift negatively, an effect that becomes more pronounced as the rate of the chemical regeneration increases. This peak shift stems from the need to sustain electron transfer under non-equilibrium surface conditions where the reduced intermediate is being depleted as fast as it is generated. A more negative potential must be applied to drive continued reduction in the face of ongoing catalytic consumption. The result of these sequence of events is a transformation in the voltammetric response: from a single, overlapping wave to a pair of well-resolved peaks, each corresponding to a separate electron transfer event. This evolving peak structure serves as a hallmark of systems governed by an EEC′ mechanism with inverted redox potentials. By framing the behavior of inverted potential systems within the EEC′ mechanism and analyzing their responses via square-wave voltammetry, we uncover the crucial role that kinetics play in shaping observable electrochemical signals. It is important to emphasize that in systems characterized by inverted potentials, a scenario may arise in which the initial electron transfer step becomes involved in a regenerative chemical reaction. Under such conditions, the overall voltammetric response may exhibit characteristics typical of a two-electron, one-step regenerative (EC') electrochemical mechanism. Effectively, the system is transformed into a simplified EC' process, wherein both electrons contribute to a concerted electrode transformation. Additionally, since the model presumes the formation of a stable intermediate species (often a radical) following the first electron transfer, in real experimental scenario there exists the possibility that this intermediate may undergo a dimerization reaction. In such a scenario, the overall electrochemical mechanism transitions into an ECEC' pathway, where the intermediate chemical step "C" represents a second-order homogeneous reaction. To the best of our knowledge, this mechanistic sequence has not yet been reported in the literature and may represent a compelling direction for future investigations in the field. The understandings from the mechanism elaborated in this work not only advances fundamental redox theory. but also enhances our ability to characterize and exploit complex redox-active species, ranging from transition metal complexes to biological cofactors such as iron–sulfur clusters, quinones and flavonoids [2,30], and other biologically relevant systems [31,32]. Ultimately, this theoretical framework enables the design of specific experiments and the development of more precise interpretive models, contributing to both analytical electrochemistry and the broader field of redox-driven chemical and biological systems.

In summary, the dimensionless rate parameter for the regenerative chemical step, defined in our model as Kchem = kc′ × c(Y)/f, highlights the critical interplay between chemical kinetics and experimental conditions in the analysis of redox systems with inverted potentials. Given that the square-wave frequency (f) influences all rate parameters in the EEC′ model, including KET,1, KET,2 and Kchem, it becomes essential to decouple these effects through careful experimental design. Specifically, modulating the concentration of the regenerative agent "Y" provides a controlled means to isolate and investigate the kinetic contribution of the chemical regeneration step. Such an approach is key to accurately interpreting square-wave voltammetric responses and discerning the underlying behavior of inverted potential systems, as illustrated in Figures 7 and 8. This strategy enables more reliable identification of mechanistic features and offers a robust pathway for characterizing complex electrochemical systems with inverted potentials via the features of an EEC′ mechanism.

Acknowledgments

Rubin Gulaboski thanks the Alexander von Humboldt Foundation (Germany) for the support via project with Ref 3.4-1070534-MKD–IP. All authors thank the Goce Delcev University, Stip, Macedonia, for the permanent support.

Declarations of interest

The authors declare no conflict of interest in this reported work.

REFERENCES

[1] C. Batchelor-McAuley, and R.G. Compton, J. Electroanal. Chem. 669 (2012) 73.

[2] M. Quan, D. Sanchez, M.F. Wasylkiw, and D.K. Smith, J. Am. Chem. Soc. 129 (2007) 12847.

[3] R. Gulaboski, V. Markovski, and J. Zhu, J. Solid State Electrochem. 20 (2016) 3229.

[4] D. Nolfi-Donegan, A. Braganza, and S. Shiva, Redox Biol. 37 (2020) 101674.

[5] F.A. Armstrong, in: A.E. Cho, W.A. Goddar III (Eds.), Metallo Proteins: Theory, Calculations and Experiments, CRC Press, Taylor & Francis Group, London, New York, USA (2015).

[6] M. Lopez-Tenes, J. Gonzalez, and A. Molina, J. Phys. Chem. C 118 (2014) 12312.

[7] F.A. Armstrong, in: A.J. Bard, M. Stratmann, G.S. Wilson (Eds.), Encyclopedia of Electrochemistry, Wiley-VCH, Weinheim (2020).

[8] J.M. Saveant, and C. Costent, Elements of Molecular and Biomolecular Electrochemistry: An Electrochemical Approach to Electron-Transfer Chemistry, 2nd Ed., John Wiley & Sons (2019).

[9] R.G. Compton, and C.E. Banks, Understanding Voltammetry, 2nd Ed., Imperial College Press, London (2011).

[10] R. Gulaboski, and V. Mirceski, Electrochim. Acta 167 (2015) 219.

[11] R. Gulaboski, and L. Mihajlov, Biophys. Chem. 155 (2011) 1.

[12] M. Lovric, and S. Komorsky-Lovric, Int. J. Electrochem. 9 (2014) 433.

[13] R. Gulaboski, and V. Mirceski, J. Solid State Electrochem. 25 (2021) 2893.

[14] A. Molina, M.M. Moreno, C. Serna, M. Lopez-Tenes, J. Gonzalez, and N. Abenza, J. Phys. Chem. C 111 (2007) 12446.

[15] V. Mirceski, S. Komorsky-Lovric, and M. Lovric, in: F. Scholz (Ed.), Square-Wave Voltammetry, Theory and Application, Springer, Berlin (2007).

[16] V. Fourmond, E.S. Wiedner, W.J. Shaw, and C. Leger, J. Am. Chem. Soc. 141 (2019) 11269.

[17] R. Gulaboski, M. Lovric, V. Mirceski, I. Bogeski, and M. Hoth, Biophys. Chem. 138 (2008) 130.

[18] R. Gulaboski, and S. Petkovska, Anal. Bioanal. Electrochem. 10 (2018) 566.

[19] A.J. Bard, and L.R. Faulkner, Electrochemical Methods: Fundamentals and Applications, Wiley, New York (2001).

[20] J.A. Osteryoung, and R. Osteryoung, Anal. Chem. 57 (1985) 101.

[21] D.H. Evans, and K. Hu, J. Chem. Soc. Faraday Trans. 92 (1996) 3983.

[22] N.A. Macias-Ruvalcaba, and D.H. Evans, J. Phys. Chem. B 110 (2006) 5155.

[23] H. Sies, and L. Parker, in: Methods in Enzymology, Academic Press, London, UK, (2004).

[24] D. Deamer, Curr. Opin. Electrochem. 29 (2021) 100742.

[25] K. Parey, C. Wirth, J. Vonck, and V. Zickermann, Curr. Opin. Struct. Biol. 63 (2020) 1.

[26] O. Haapanen, and V. Sharma, Curr. Opin. Electrochem. 29 (2021) 100741.

[27] M.A. Hagras, and A.A. Stuchebrukhov, J. Phys. Chem. B 123 (2019) 5265.

[28] C. Hessin, J. Schleinitz, N. Le Breton, S. Choua, L. Grimaud, V. Fourmond, M. Desage-El Murr, and Ch. Léger, Inorg. Chem. 62 (2023) 3321.

[29] M. Janeva, P. Kokoskarova, and R. Gulaboski, Anal. Bioanal. Electrochem. 12 (2020) 766.

[30] I. Bogeski, R. Gulaboski, R, Kappl, V. Mirceski, M. Stefova, J. Petreska Stanoeva, and M. Hoth, J. Am. Chem. Soc. 133 (2011) 9293.

[31] B.D. Fleming, J. Zhang, A.M. Bond, S.G. Bel, and L.L. Wong, Anal. Chem. 77 (2005) 3502.

[32] B.A. Kovert, L. Marcoux, and A. J. Bard, J. Am, Chem. Soc. 94 (1972) 5538.